Metallobiochemistry of ultratrace levels of bismuth in the rat

I. Metabolic patterns of $^{205+206}Bi^{3+}$ in the blood

Enrico Sabbioni[1,3], Flavia Groppi[2,3], Mario Di Gioacchino[1,4], Claudia Petrarca[1,5], Simone Manenti[2,3]*

1. Center for Advanced Studies and Technology (C.A.S.T.), "G. d'Annunzio" University of Chieti-Pescara, Via Luigi Polacchi 11, Chieti, I-66100, Italy

2. Department of Physics, Università Degli Studi di Milano, Via Celoria 16, Milano, I-20133, Italy

3. LASA, Department of Physics, Università Degli Studi di Milano and INFN-Milano, Via F.lli Cervi 201, Segrate (MI) I-20090, Italy

4. Institute of Clinical Immunotherapy and Advanced Biological Treatments, Piazza Pierangeli 1, Pescara; Rectorate of Leonardo da Vinci Telematic University; Largo San Rocco 11 Torrevecchia Teatina, CH, Italy

5. Department of Medicine and Aging Sciences, "G. d'Annunzio" University of Chieti-Pescara, via Luigi Polacchi 11, Chieti, I-66100, Italy

*Corresponding author: simone.manenti@unimi.it; simone.manenti@mi.infn.it

Abstract

Background: The number of the applications of bismuth (Bi) is rapidly and remarkably increasing, enhancing the chance to increase the levels to which humans are normally daily exposed. The interest to Bi comes also from the potential of Bi-based nanoparticles (BiNPs) for industrial and biomedical purposes. Like other metal-based NPs used in nanomedicine, BiNPs may release ultratrace amounts of Bi ions when injected. The metabolic fate and toxicity of these ions still needs to be evaluated. At present, knowledge of Bi metabolism in laboratory animals refers almost solely to studies under unnatural "extreme" exposures, i.e. pharmacologically relevant high-doses (up to thousand mg kg^{-1}) in relation to its medical use, or infinitesimal-doses (pg kg^{-1} as non-carrier-added Bi radioisotopes) for radiobiology protection, diagnostic and radiotherapeutic purposes. No specific study exists on the "metabolic patterns" in animal models

exposed to levels of Bi, i.e. at “environmental dose exposure” that reflect the human daily exposure (µg kg^{-1}).

Methodology: Rats were intraperitoneally injected with 0.8 µg Bi kg^{-1} bw as $^{205+206}Bi(NO)_3$ alone or in combination with ^{59}Fe for radiolabelling of iron proteins. The use of $^{205+206}Bi$ radiotracers allowed the detection and measurement down to pg fg^{-1} of the element in the blood biochemical compartments and protein fractions as isolated by differential centrifugation, size exclusion- and ion exchange chromatography, electrophoresis, solvent extraction, precipitation and dialysis.

Results: 24 h after the administration, the blood concentration of Bi was 0.18 ng mL^{-1}, with a repartition plasma/red blod cells (RBC) in a ratio of 2:1. Elution profiles of plasma from gel filtration on Sephadex G-150 showed four pools of Bi-binder proteins with different molecular sizes (> 300 kDa, 160 kDa, 70 kDa and < 6.5 kDa). In the 70 kDa fraction transferrin and albumin were identified as biomolecule carriers for Bi. In red blood cells, Bi was distributed between cytosol and membranes (ghosts) in a ratio of about 5:1. In the cytosol, low molecular components (LMWC) and the hemoglobin associated the Bi in a ratio of about 1.8:1. In the hemoglobin molecule, Bi was bound to the beta polypeptide chain of the globin. In the ghosts, Bi was detected at more than one site of the protein fraction, with no binding with lipids. Dialysis experiments and the consistently high recovery (80-90%) of ^{206}Bi from chromatography of ^{206}Bi-containing biocomponents suggest that Bi was firmly complexed at physiological pH with a low degree of breaking during the applications of experimental protocols for the isolation of the ^{206}Bi-biocomplexes. These latter were sensitive to acid buffer pH 5, and to the presence of complexing agents in the dialysis fluid.

Conclusions: On the basis of an environmental biochemical toxicology approach, we have undertaken a study on the metabolic patterns of Bi^{3+} ions in rats at tissue, subcellular and molecular level with the identification of cellular Bi-binding components. As a first part of the study the present work reports the results concerned with the metabolic fate of ultratrace levels of $^{205+206}Bi(NO)_3$ in the blood.

Keywords

Bismuth; Radioisotopes; Environmental toxicology; Metabolic pattern; Rat blood

1. Introduction

Bismuth (Bi, atomic number 83) is a heavy metal of the Group VA in the periodic table along with arsenic and antimony. Ubiquitous in the environment and without a known biological function, it forms compounds mainly in oxidation state 3+.

The use of Bi has grown rapidly in the last decades. There are more than 100 commercial Bi-containing products from industrial to pharmaceutical products [1].

In modern industry, due to the low toxicity to humans, Bi has the status of an ‘‘amazingly ‘green’, environmentally-minded element’’ [2] which explains why it is widely used as replacement for toxic lead-containing products, i.e. brass plumbing fixtures, fishing sinkers, free machining steels, solders, shotgun pellets and metallurgical additives in foundries. Bi-vanadate and Bi-telluride-based materials are highly promising for high efficiency-energy applications [3]. Bi is used as a catalyst in the oxidation/ammoxidation of lower olefins, one of the most important industrial processes [4]. Ceramic glazes, lubricating greases, and crystal ware are manufacture applications while in cosmetics, Bi is considered a pearlescent agent, producing a high shine in nail polishes, lipsticks, and eye shadows [5].

In medicine, Bi has been used for more than 200 y, i.e. for the treatment of skin lesions, syphilis, colitis, and parasite infections [6]. Its use drastically decreased after episodes of encephalopathy in mid-seventies in France and Australia in relation to long-term treatment with high doses of Bi-salicylate [7]. The main use of Bi- drugs today lies in the treatment of *Helicobacter pylori* associated peptic ulcers and gastrointestinal disorders [8,9]. However, recent i*n vitro* studies showed antifungal and anticancer activity of Bi-complexes [5] as well as an antiviral action, being ranitidine Bi citrate complex effective in inhibiting the severe acute respiratory syndrome coronavirus (SARS-CoV) helicase, with strong reduction of the virus replication [10]. Moreover, the alpha emitters radiobismuth ^{212}Bi ($t_{½}$=1 h) and ^{213}Bi ($t_{½}$=45.6min) have been used as targeted radiotherapeutic agents for cancer therapy [11].

Very recently the potential of Bi-based nanoparticles (BiNPs) in industry [12] and nanomedicine [13] increased the interest in Bi applications. BiNPs are a unique category of materials that possess excellent

chemical, electrical, optical, and catalytic activities. They are used in photocatalytic degradation processes [14] and have been proposed as pigment and ceramic materials [15], a substitute for Pb-based nanoparticles in the piezoelectric industry [16] and potential UV filters in cosmetics [17]. Moreover, potential applications of BiNPs are emerging in nanomedicine, including drug delivery, combined cancer therapy [18], photothermal and radiation therapy [19], bioimaging [20], theranostics [21], antibacterial use [22], tissue engineering [23], biosensing [24] and shielding applications [25].

We expect that the growing interest for Bi applications will enhance the chance to increase the environmental levels of Bi to which humans are normally daily exposed. In this context, the knowledge of the physiological metabolic pathways of Bi in experimental animal models, i.e. at ultratrace level of exposure, is essential for the proper evaluation of the health risk. Analysis of the literature on Bi metabolism in animal models indicates the following: (i) the long history of the use of Bi- drugs has oriented the research towards pharmacological aspects. Laboratory animals have been exposed to high doses (ten to thousands mg kg^{-1} bw), falling in the category of acute/subacute exposure with induction of neurotoxicity, renal failure and bone diseases [26]; (ii) much less data, mostly obtained decades ago, have been gathered from diagnostic, radiobiology protection and radiotherapy research. In such studies laboratory animals were mostly exposed to infinitesimal doses (no-carrier-added (NCA) Bi-radiotracers, typically pg kg^{-1} bw) [27,28,29,30]; (iii) no toxicology study has been carried out at environmental exposure levels (of the order of µg kg^{-1} bw [31]), to which humans are exposed on a daily basis. Thus, from this point of view, the metabolism of Bi remains obscure.

To fill this gap, we have undertaken a study of the metabolic patterns of Bi in rats at tissue, subcellular and molecular level with the identification of cellular Bi-binding components. The present work is the first part of the study and concerns a still controversial issue such as the metabolic fate of Bi in the blood. The study was made possible by using very high sensitive radioanalytical techniques, i.e. using $^{205+206}$Bi radiotracers for the labelling of ultratrace levels of Bi, in combination with biochemical techniques for cellular fractionation [32].

2. Materials and methods

2.1. Chemicals, reagents and equipment

All chemicals were analytical reagent grade or better (Sigma Aldrich, Milan, Italy). Milli-Q purified water (Millipore) was used throughout. Metallic lead (Pb) foils (purity 99.99%) for cyclotron activation were obtained from Goodfellow Metals (Prodotti Gianni, Milan, Italy). Sephadex G-150, G25 and DEAE Sephadex A-50 resins were supplied by Pharmacia, Uppsala, Sweden; blue Dextran and proteins with known molecular weight for pre-calibration of Sephadex column as well as carboxymethyl CM-cellulose (Whatman CM32) by Sigma Aldrich (Milan, Italy); Visking semi-permeable tubing by Serva, SERVA, Heidelberg (Germany). 2-mercaptoethanol, urea, EDTA, meso-dimercaptosuccinic acid (DMSA), citrate, Trizma base, sodium cacodylate, sodium phosphate and Amido black staining solution were purchased from Sigma Aldrich (Milan, Italy); sodium dodecylsulphate (SDS) from BioRad Lab (Milan, Italy).

The used equipments were: TL-100 refrigerated ultracentrifuge (Beckmann Instrument, Palo Alto , CA) and Eppendorf centrifuge 5810 R (Eppendorf, Milano, Italy); Potter-Elvehjem PTFE pestle and glass tube (Braun, Melsungen, Germany); Lambda 25 double-beam spectrometer for UV/Vis range (Perkin-Elmer, Milan Italy); Ultrorac fraction collector 7000 and Uvicord II (LKB Produkter, Stockholm, Sweden); Mini-PROTEAN electrophoresis chamber and PowerPac™ Basic power supply (Bio-Rad, Segrate, Milano, Italy); home-made completely automatic dialysis system for the simultaneous dialysis at +4°C of 12 samples per day.

2.2. Radiolabels

NCA radioactive Bi was prepared at the Scanditronix MC40 cyclotron [33] by 30 MeV proton bombardment of a natural metallic Pb target [34]. Under our experimental conditions a mixture of $^{205+206}$Bi ($t_{1/2}$= 15.3 d and 6.24 d, respectively) were formed, having been radiochemically separated by dissolving the irradiated Pb target in 3 mol L^{-1} HNO_3 followed by Pb precipitation and anion exchange chromatography on Dowex1x8 (yield near to 90%, [35]). At the time of the use, the characteristics of $^{205+206}$Bi solution (hereinafter simply referred as ^{206}Bi) were: 2 mCi (74 Mbq) mL^{-1}; radiochemical purity: > 99% (by paper

chromatography in butanol-water thiocyanic solution); radionuclidic purity: > 99% (by ^{206}Bi decay and gamma spectra); chemical impurities: < 1 µg mL^{-1} (by Instrumental Neutron Activation Analysis – INAA, Atomic Absorption Spectroscopy – AAS and Inductively Coupled Plasma Mass Spectrometry – ICP-MS); specific radioactivity: 14 µCi ng^{-1} Bi as determined by pre-concentration on Chelex 100 column [36], elution with 2 mol L^{-1} HNO_3 followed by ICP-MS [37]; final chemical form: isotonic solution of $Bi(NO)_3$ pH 5.6, sterilized by filtration (recovery of ^{206}Bi > 88%).

$^{59}FeCl_3$ (specific activity 4.5 µCi (0.167 MBq) μg^{-1} Fe) was purchased from the Radiochemical Centre, Amersham, UK.

2.3. Radioactive counting

Measurements of ^{206}Bi were carried out by integral γ-counting with a Wizard 3 Gamma Counter apparatus (Perkin Elmer, Life Sciences) equipped with a well-type 3.15" x 3" NaI(Tl) size crystal (4π counting geometry for optimal counting efficiency), and performance up to 2 048 keV [38]. Since ^{206}Bi was not in the radioisotope library for automatic calibration we carried out a manual calibration. In this context, an aliquot of the ^{206}Bi solution to be injected into animals (mother solution) was placed in the counter to obtain the γ-ray spectrum from which the main γ-peaks, the lower and upper energy levels were determined. The interval 100 – 2 000 keV was used to set an appropriate energy threshold and windows for our experimental conditions. Radioactivity measurements of ^{206}Bi were interpreted in terms of exogenous element concentrations by comparison with ^{206}Bi reference solutions (aliquots of the same radioactive mother solutions administered to animals).

In double labelled experiments ^{206}Bi and ^{59}Fe were simultaneously measured by computer-based γ-ray spectrometry using a HPGe detector (EG&G Ortec Int,GA,USA) [39]. The characteristic photon emissions of 803 keV (^{206}Bi) and 1 298 keV (^{59}Fe) were used.

2.4. Animals and treatment

Male Sprague-Dawley rats (250 ± 20 g, Harlan Nossan, Correzzana. Italy) were individually kept in metabolic cage (200 cm^2, Techniplast, Gazzada, Italy) in temperature (23 ± 2°C), humidity (50 ± 10%), ventilation and light-dark-controlled room. Animals were accustomed to our housing conditions for one week before being used. They were maintained with commercial food in pellets and natural mineral water (Acqua Panna, Tuscania, Italy) *ad libitum*. Housing conditions and experimental procedures were in strict accordance with the European Community regulations [40]. Exposure of the animals and their treatment were carried out in two steps.

In the first step, five animals were intraperitoneally (i.p.) injected with a single dose of Bi (0.8 µg Bi kg^{-1} bw) as $Bi(NO)_3$ plus 46.8 µCi (1.73 MBq) of ^{206}Bi/rat in the same chemical form.

In the second step, three animals were individually i.p. injected with 52 µCi (1.92 MBq) of $^{206}Bi(NO)_3$ (0.89 µg Bi kg^{-1} bw) together with 1.2 µg Fe^{3+} as chloride plus 10 µCi (0.37MBq) of ^{59}Fe in the same chemical form.

2.5. Blood collection and fractionation

24 h after dosing the rats were anaesthetized with Nembutal (40 mg kg^{-1} bw) and sacrificed by cardiac puncture. Blood was collected with a heparinized syringe, centrifuged at 2 500 g for 15 min to separate plasma and RBC that were counted for the ^{206}Bi content and further fractionated into biochemical components (Fig.1).

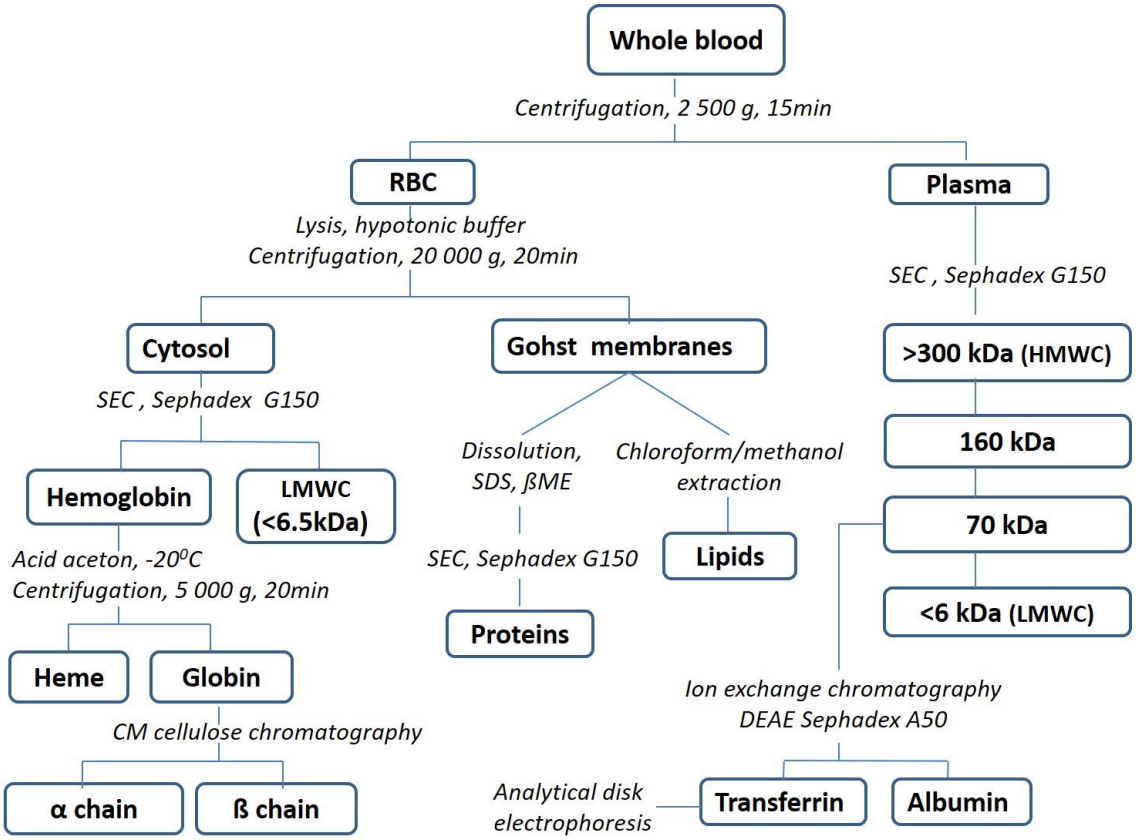

Fig.1 Flow diagram of the fractionation of the rat blood into sub compartments and biochemical components. For details see Sections 2.6 and 2.7. SEC: Size Exclusion Chromatography; SDS: Sodium Dodecyl Sulphate; ßME: β-mercaptoethanol; CM: Carboxymethyl; DEAE: Diethylaminoethyl; LMWC: Low Molecular Weight Components; HMWC: High Low Molecular Weight Components

2.6. Plasma fractionation

Separation of plasma proteins was carried out by size exclusion chromatography (SEC) on a Sephadex G-150 column (2.5 cm x 100 cm) pre-calibrated with a kit of standard proteins with known molecular weight and equilibrated with 10 mmol L^{-1} cacodylate buffer, pH 7.2 [41]. Each fraction of the eluate was analyzed for the ^{206}Bi radioactivity and the UV profile recorded at 280 nm. At this wavelength, the amino acids tryptophan and tyrosine and to a lesser extent cysteine residue exhibit strong light absorption [42], becoming the measurement at 280 nm the most common, fast, and reproducible method for determining protein profiles in SEC. The ^{206}Bi- containing fractions of the eluate with a molecular weight (MW) approx. of 70 kDa were pooled, desalted on a Sephadex G-25 column, freeze-dried, dissolved in 10 mmol L^{-1} Tris buffer, pH 8.0, and submitted to ion exchange chromatography on a DEAE-Sephadex A-50 column (1.5 cm x 25 cm) to separate

transferrin and albumin fractions [38]. Proteins and ^{206}Bi in the eluate were monitored spectrophotometrically at 280 nm and γ-counting, respectively.

2.7. RBC fractionation

2.7.1. Separation of RBC membranes (ghosts) and cytosol was performed by washing the packed RBC with isotonic buffer (0.9% saline, 5 mmol L^{-1} sodium phosphate, pH 8) followed by lysis in a hypotonic buffer (5 mmol L^{-1} sodium phosphate, pH 8, without NaCl) [43]. The pellets (membranes or ghosts) were separated from the red hemolysate (cytosol) by centrifugation (20 000 g for 20 min), washed with the hypotonic buffer until the supernatant became colorless (complete removal of hemoglobin and enzymes) and ^{206}Bi counted in the ghost and cytosol fractions.

2.7.2. Separation of lipids from the ghost fraction was carried according to the method of Folch [44]. The ghosts were homogenized with 2:1 v/v chloroform-methanol mixture in a Potter-Elvehjem homogenizer. The homogenate was stirred for 15 min in an orbital shaker at room temperature and then filtered on a paper Whatman No. 1. The recovered liquid phase was washed with 0.2 volume of water to induce phase separation and the mixture was centrifuged at 1 000 g for 10 min to separate the two phases. The alcoholic layer (upper phase) was removed by aspiration. The chloroform layer (lower phase) contained the lipids. ^{206}Bi was counted in both phases.

2.7.3. Fractionation of ghost proteins was carried out on aliquots of the nondelipidated membranes according to Bornens [45] with minor modifications. The proteins of the ghosts were solubilized for 20 min with 2% sodium dodecylsulfate (SDS) solution, 0.1% 2-mercaptoethanol, 5 mmol L^{-1} phosphate buffer, pH 7.2. The solubilized samples were incubated at 37°C for 15 min. Any insoluble material was separated by ultracentrifugation (105 000 g, 1 h). The dissolved membranes were dialyzed against the solubilizing buffer and then layered onto Sephadex G-150 column (2.5 cm x 100 cm) previously equilibrated with the same buffer. The eluate was monitored online for proteins at 280 nm and the ^{206}Bi counted in each fraction.

2.7.4. Fractionation of RBC cytosol was carried out by SEC on Sephadex G-150 column (1.6 cm x 100 cm) previously calibrated and equilibrated with 5 mmol L^{-1} phosphate buffer, pH 8.0. The UV profile of the eluate was recorded at 540 nm to determine the position of the hemoglobin (Hb) peak [46] and the ^{206}Bi measured in each fraction.

2.7.5. Separation of heme and globin was achieved as described in [47] with few adaptations. The Hb- containing fractions from the Sephadex G-150 of the cytosol (see Section 2.7.4) were pooled, dialyzed against distilled water and pre-cooled at -20°C. 5 mmol L^{-1} of the pre-cooled Hb solution was treated with acid acetone (0.006 mol L^{-1} HCl) at -20°C. The supernatant (heme, red fraction) was separated from the pellet (globin, white precipitate) by centrifugation at 5 000 g at 4°C for 20 min. The globin pellet was washed with 50 mL pre-cooled acid acetone. The step was repeated thrice. The ^{206}Bi was counted in both heme and globin fractions.

2.7.6. Separation of α and ß peptide chains of globin was performed by CM-cellulose chromatography with small adaptations [48]. A freshly acetone-precipitated ^{206}Bi-containing globin was dialyzed for 3 h in a starting buffer (5 mmol L^{-1} Na_2HPO_4 and 50 mmol L^{-1} 2-mercaptoethanol in 8 mol L^{-1} urea solution, pH 6.8), dissolved for 24 h in the same buffer and applied on CM-cellulose column (1 cm x 15cm) previously equilibrated with the starting buffer. 50 mL of the starting buffer were flowed through the column in order to remove any unbound material. The globin chains were eluted using a gradient of 0.005-0.05 mol L^{-1} Na_2HPO_4, pH 6.7. Proteins of the eluted fractions were monitored at 280 nm and ^{206}Bi counted in each fraction.

2.8. Dialysis experiments

1 to 3 mL of samples were introduced in Visking semi-permeable membrane tubing (MW cut off 12 - 14 kDa) and dialyzed for 24 h against three changes of 2 L of: (i) buffers used for sample separation, alone or containing chelating agents (EDTA, DMSA or citrate); (ii) 10 mmol L^{-1} acetate buffer, pH 5.0. The ^{206}Bi was measured in the membrane tubing before and after dialysis. As a control, ^{206}Bi radiotracer

solution alone was dialyzed against the different buffers considered, and the percent radioactivity retained in the tubing was determined.

2.9. Isolation of [^{206}Bi + ^{59}Fe]- double labelled transferrin

In the first step of the study a ^{206}Bi-containing transferrin fraction was isolated from the plasma by SEC on Sephadex G-150 followed by anion exchange chromatography on DEAE Sephadex A50 of the pooled 70 kDa fractions (see above, section 2.6 Plasma fractionation). To strengthen further the ability of Bi to bind transferrin, a second group of rats was simultaneously administered with ^{206}Bi and ^{59}Fe for the radiolabeling of iron proteins. Then, the [^{206}Bi+^{59}Fe]-containing blood plasma was separated from RBC and fractionated by SEC on Sephadex G150 and DEAE-Sephadex A-50 as described in the section 2.6 Plasma fractionation. The [^{206}Bi+^{59}Fe]-transferrin containing fractions from DEAE column, identified by γ-ray spectrometry, were pooled, concentrated by ultrafiltration and submitted to analytical disc electrophoresis (7.5% acrylamide gel, Tris-glycine, pH 9, 2 mA/tube at 4°C). Samples were made in duplicate. The first gel was monitored for proteins by Amido black staining at 620 nm. The second was sliced into disks 2 mm thick using a razor blade slicer, which were analyzed for ^{206}Bi and ^{59}Fe content by γ-ray spectrometry. As a control, the electrophoretic pattern of ^{206}Bi-nitrate alone was determined.

2.10. Statistical treatment

All figures and statistical analyses were performed using the software OriginPro, Version 2020 (OriginLab Corporation, Northampton, MA, USA). A two-sided p-value < 0.01 was used to indicate statistical significance.

Experiments were conducted in three or five replicates and the final values were expressed as mean ± standard deviation (SD).

3. Results

3.1. Distribution in the blood

In the circulatory system, 24 h after i.p. injection with 0.8 µg Bi kg^{-1} bw as $^{206}Bi(NO)_3$ the concentration of Bi in the blood was less than 0.2 ng Bi mL^{-1} (Table 1). The content of Bi in the blood of 3 unexposed rats (control group) was < 0.03 ng mL^{-1} as measured in our laboratory by ICP-MS (SCIEX ELAN DRCII equipped with a Dynamic Cell Reaction, Perkin Elmer, Turhill, Ontario, Canada). A significant statistical difference in whole blood Bi content was observed between the exposed and unexposed rats ($p < 0.01$).

Separate analysis of the packed RBC and supernatant plasma after centrifugation showed that two thirds of the blood Bi was present in the plasma and one third in the erythrocytes (Table 1).

Table1. Concentration of Bi in whole blood, plasma and erythrocytes of rats after 24 h of i.p. injection of 0.8 µg Bi kg^{-1} bw as $^{206}Bi(NO)_3$ [a].

Blood compartment	Bi content	
	%dose mL^{-1}	**ng Bi mL^{-1}**
Whole blood	0.09 ± 0.02	0.18 ± 0.05
Plasma	0.06 ± 0.02	0.12 ± 0.04
RBC	0.03 ± 0.01	0.06 ± 0.02

a: mean of 5 animals ± SD

3.2. Fractionation of the ^{206}Bi-containing plasma

The primary understanding of the Bi-binding constituents of rat plasma was achieved by *SEC* on Sephadex G-150. Four peaks of radioactivity emerged in the eluate (Fig.2) all in association with UV absorbing components and with different percentage breakdown of the ^{206}Bi in each peak: (i) a minor peak I, emerging beyond the void volume of the column in the region of high molecular weight components (> 300 kDa, HMWC); (ii) a major peak II, corresponding to the fraction with apparent molecular weight of 160 kDa; (iii) peaks III and IV, eluted approx. in the 70 kDa and < 6.5 kDa, corresponding to transferrin/albumin and low molecular weight components (LMWC) fractions, respectively. The further resolution of the 70 kDa fraction (transferrin/albumin) by chromatography on DEAE Sephadex A-50 (Fig.3) and counting of ^{206}Bi in each fraction showed that Bi eluted in association with both transferrin and albumin UV peaks in a ratio of about 3:1 (Table 2). The binding of ^{206}Bi with transferrin was definitively

confirmed by ^{206}Bi+ ^{59}Fe-double labelled experiments (see Section 2.9). Fig.4 illustrates the results of the analytical disk electrophoresis of the [^{206}Bi+^{59}Fe]-double-labelled transferrin fraction isolated by SEC of plasma of rats injected with [^{206}Bi+^{59}Fe], followed by DEAE Sephadex A-50 chromatography (chromatography profiles not shown, see Section 2.9). ^{206}Bi and ^{59}Fe revealed coincident peaks of radioactivity in the electrophoretic gel, suggesting transferrin as *in vivo* Bi-binding protein of the rat blood.

Table 2. Relative distribution of Bi among blood components of rats 24 h after i.p. injection of 0.8 µg Bi kg^{-1} bw as ^{206}Bi (NO)$_3$[a]. See Fig. 1 for the procedures used to separate the sub-compartments.

Compartment	Sub-compartment	^{206}Bi in the sub-compartment (% of the total ^{206}Bi of the compartment)[b]
Whole blood:		100
	Plasma	67 ± 2.6
	RBCs	33 ± 3.8
Whole Plasma:		100
	>300 kDa (HMWC)[c]	5
	160 kDa[c]	55
	70 kDa[c]	30
	<6.5 kDa (LMWC)[c]	10
70 kDa:		100
	transferrin[d]	75
	albumin[d]	25
Whole RBC:		100
	ghost	16 ± 3.5
	cytosol	84 ± 5.8
RBC ghosts:		100
	70 kDa[e]	81
	30 kDa[e]	19
	Lipids[f]	1.9 ± 1.7
RBCs cytosol:		100
	Hemoglobin (Hb)[g]	36
	LMWC (<6.5 kDa)[g]	64
Hemoglobin (Hb):		100
	heme	5 ± 2.9
	globin	95 ± 8.1
Globin:		100
	α chain[h]	<2%
	ß chain[h]	> 98%

a: mean of 5 determinations ± SD
b: recovery of ^{206}Bi in the sub compartments: from 88% to 96%. The values with no SD were derived from a single SEC experiment.
c: derived from SEC on Sephadex G-150 (Fig.2)
d: derived from DEAE Sephadex A-50 chromatography (Fig.3)
e: derived from SEC on Sephadex G-150 of non-delipidated membranes (Fig.4)
f: from chloroform-methanol extraction on native membranes [44]
g: derived from SEC on Sephadex G-150 (Fig.5). LMWC: low molecular weight components.
h: derived from CM cellulose chromatography (Fig.6)

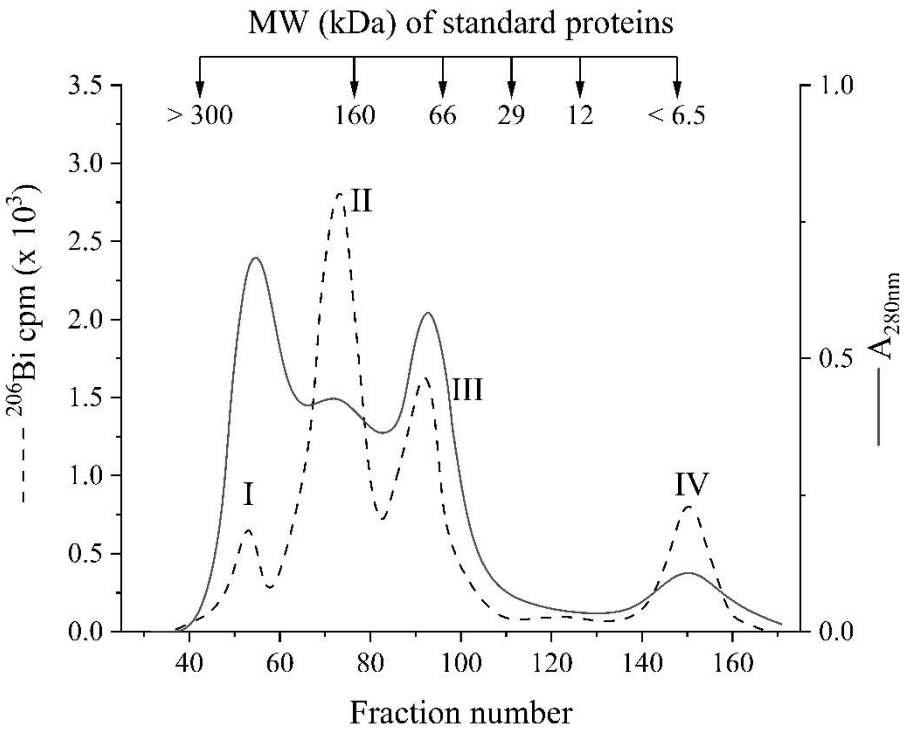

Fig.2 SEC of plasma proteins of rats 24 h after i.p. injection of 0.8 µg Bi kg^{-1} bw as $^{206}Bi(NO)_3$. Aliquots of ^{206}Bi-containing plasma were layered onto a Sephadex G-150 column previously equilibrated with 10 mmol L^{-1} sodium cacodylate–HCl buffer, pH 7.2 and eluted with the same buffer. Recovery of applied ^{206}Bi: 89%. Molecular weights (MW) were approx. deduced from standard proteins (horse spleen apoferritin, 440 kDa; rabbit muscle aldolase, 160 kDa; bovine serum albumin, 66 kDa; bovine erythrocytes carbonic anhydrase, 29 kDa; horse heart cytochrome c, 12.4 KDa, and bovine lung aprotinin, 6.5 KDa).

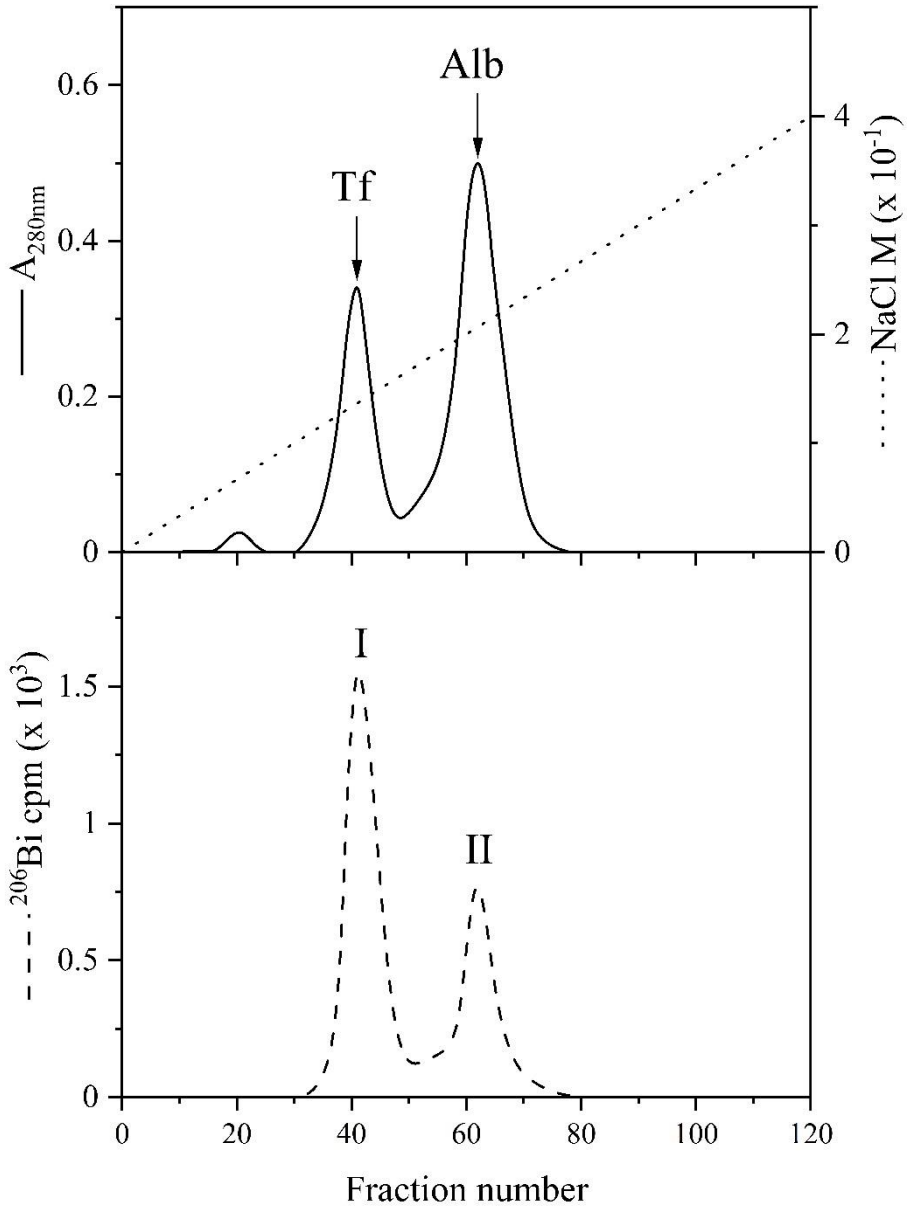

Fig.3 Anion exchange chromatography on DEAE Sephadex A-50 column (1.5 cm x 25 cm) of the pooled ^{206}Bi-containing peak III from SEC of the ^{206}Bi-plasma (Fig. 2). The loaded sample was eluted with a linear saline gradient composed of 10 mmol L^{-1} Tris, 0-0.5 mol L^{-1} NaCl, pH 8. Recovery of applied ^{206}Bi: 81%. Tf: transferrin; Alb: albumin.

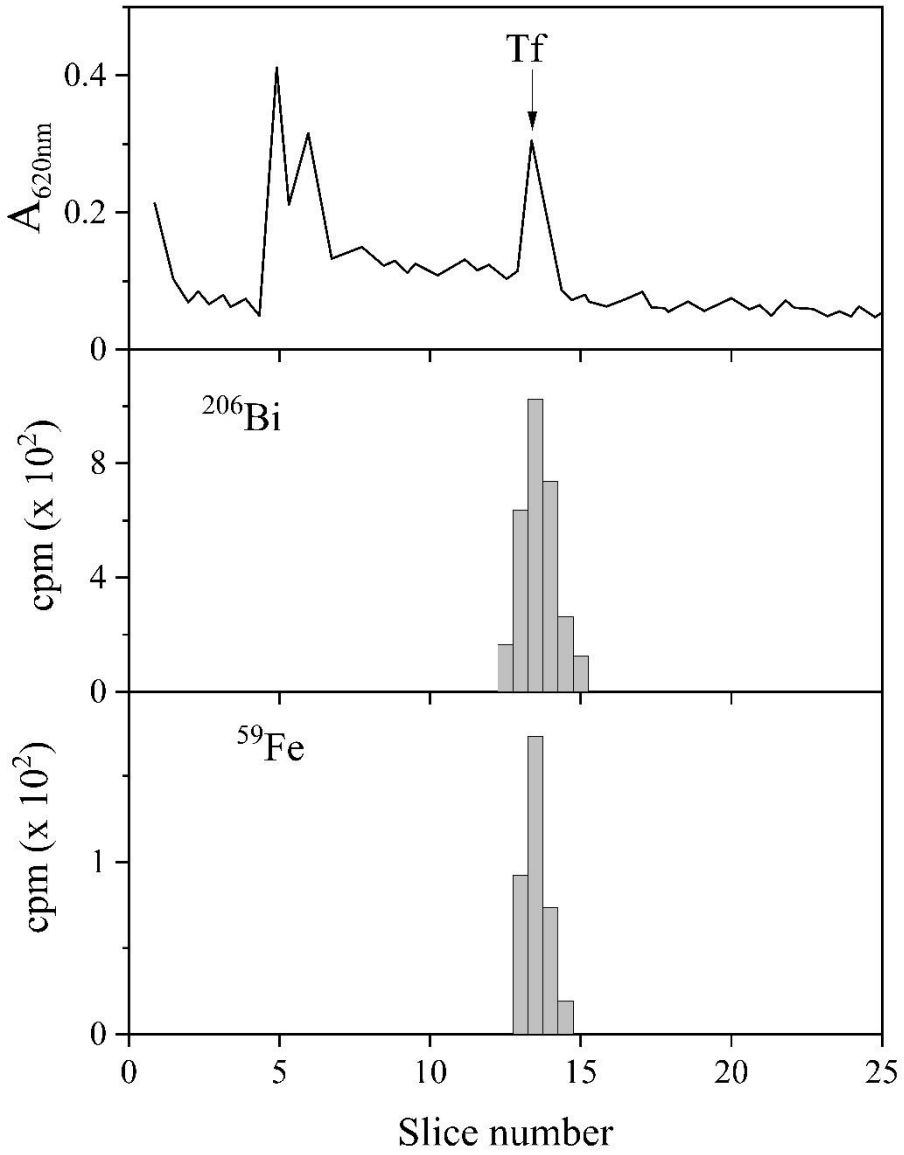

Fig.4 Electrophoretogram of the pooled ^{206}Bi+^{59}Fe- transferrin fractions from anion exchange chromatography on DEAE Sephadex A-50 (see Section 2.9). Recovery of applied radioactivity: 88 %. In the electrophoresis of ^{206}Bi alone (control) the radioactivity migrated off the end of the gel.

3.3. Fractionation of the ^{206}Bi- containing RBC

Separation of ^{206}Bi-containing erythrocytes into ghosts (membranes) and cytosol showed a prevalence of the Bi in the cytosol fraction in comparison with its association with membrane components in a ratio of about 5:1 (Table 2). Within the membrane, Bi was bound mostly entirely to proteins, being the radioactivity in the chloroform-methanol extract obtained by the Folch's method [44] (lipid fraction) less than 2% of the total Bi of the membranes (Table 2).

When an aliquot of non-delipidated membranes was dissolved in SDS-solubilizing buffer, dialyzed against the same buffer and chromatographed on Sephadex G-150 (see Section 2.7.3) the result shown in Fig.5

was obtained. ^{206}Bi was eluted in association with two UV-absorbing peaks: (i) a major peak I, (molecular size approx. of 70 kDa); (ii) a minor peak II (approx. 45 kDa), being the two peaks in a ratio of about 4:1. Dialysis experiments on non-delipidated or delipidated membranes against the solubilizing buffer indicated in both cases that only a small and mostly identical percentage of Bi was removed by dialysis at physiological pH (Table 3).

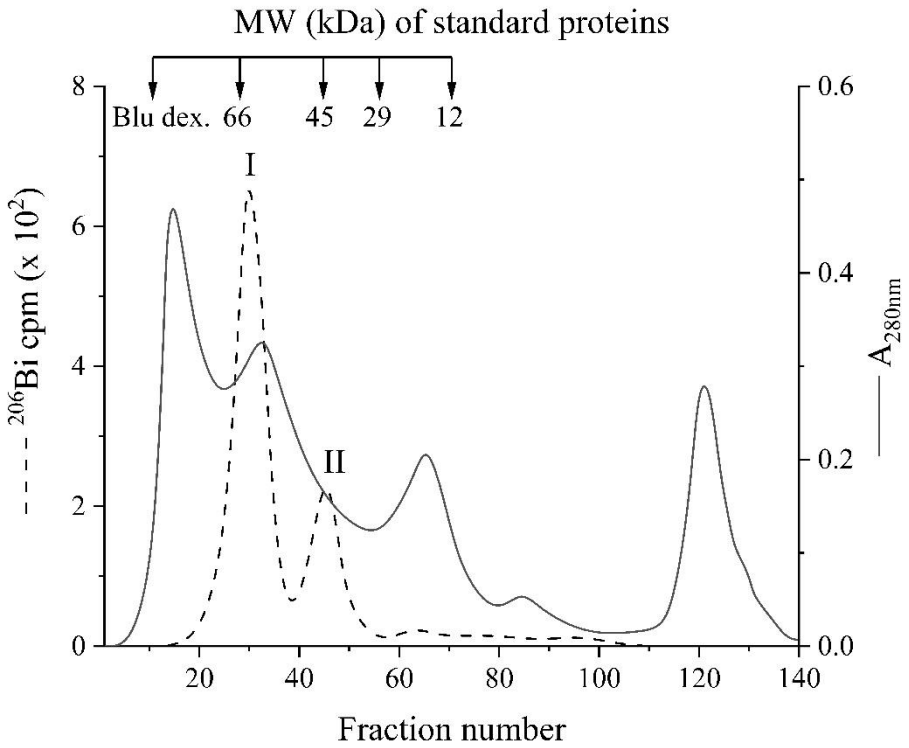

Fig.5 SEC on Sephadex G-150 (2.5 cm x 100 cm) of non-delipidated RBC membranes solubilized in 2% sodium dodecylsulfate (SDS) solution, 0.01% 2-mercaptoethanol, 5 mmol L^{-1} phosphate buffer, pH 7.2. The column was equilibrated and eluted with the same solubilizing buffer. Recovery of applied ^{206}Bi: 90%. Molecular weights (MW) were approx. deduced from standard proteins (bovine serum albumin, 66 kDa; hen egg ovalbumin, 45 kDa; bovine erythrocytes carbonic anhydrase, 29 kDa; horse heart cytochrome c, 12.4 kDa).

Table 3. Dialysis of ^{206}Bi-containing plasma, RBC and subcomponents from blood of rats 24 h after i.p. injection of 0.8 µg Bi kg^{-1} bw as ^{206}Bi (NO)$_3$ [a]

Blood component	^{206}Bi (% of the applied radioactivity retained inside the tubing at the end of dialysis)				
	Buffer of dialysis alone (A)	A+1 mmol L^{-1} EDTA	A+1 mmol L^{-1} DMSA[a]	A+1 mmol L^{-1} citrate	10 mmol L^{-1} acetate pH 5.0
Plasma					
Whole plasma	88.2 10 mmol L^{-1} cacodylate pH 7.2	22.5	4.8	15.3	8.3

Albumin [b]	87.2 10 mmol L^{-1} Tris HCl pH 8.0	21.3	3.4	16.7	7.4
Transferrin [b]	92.5 10 mmol L^{-1} Tris HCl pH 8.0	16.7	5.6	26.2	6.8
RBC					
Whole RBC[c]	80.8 5 mmol L^{-1} sodium phosphate pH 8	14.5	3.5	20.7	8.6
Non Delipidated membrane[d]	94.3 Solubilizing buffer pH 8	18.1	5.3	23.4	9.7
Delipidated membrane[e]	93.1 Solubilizing buffer pH 8	22.4	5.0	13.6	6.2
RBC cytosol[e]	64.4 5 mmol L^{-1} sodium phosphate pH 8	27.4	2.9	16	5.8
Hemoglobin[f]	93.4 5 mmol L^{-1} sodium phosphate pH 8	22.8	3.6	12.9	10
Globin[g]	90.9 10 mmol L^{-1} cacodylate pH 7.2	17.5	5.7	14.8	8.2

a: mean of 3 determinations, relative standard deviation (RSD) < 22%. In the control ($^{206}Bi^{3+}$ alone in the four types of buffers A) the applied radioactivity retained in the tubing at the end of the dialysis ranged from 4.1 to 8.4%.
b: derived from ion exchange chromatography on DEAE Sephadex A-50 (Fig.3)
c: resuspended in phosphate buffer after separation of the plasma
d, e: after separation of RBC cytosol, native (d) or after (e) lipid extraction (see Sections 2.7.1 and 2.7.2)
e: after separation of RBC ghosts (see Section 2.7.1)
f: from SEC of cytosol (Fig.5)
g: resuspended after acid acetone precipitation (see Section 2.7.5)

Chromatography of the RBC cytosol on Sephadex G-150 revealed two peaks of ^{206}Bi in the eluate (Fig.6). The minor peak I, emerged in association with the 540 nm UV peak coincident with the maxima of the total protein (A at 280 nm) corresponding to hemoglobin (Hb) fraction. The fairly large peak II was eluted in the region of LMWC (apparent MW < 6.5 kDa), being the two peaks in a ratio of about 1:1.8 (Table 2).

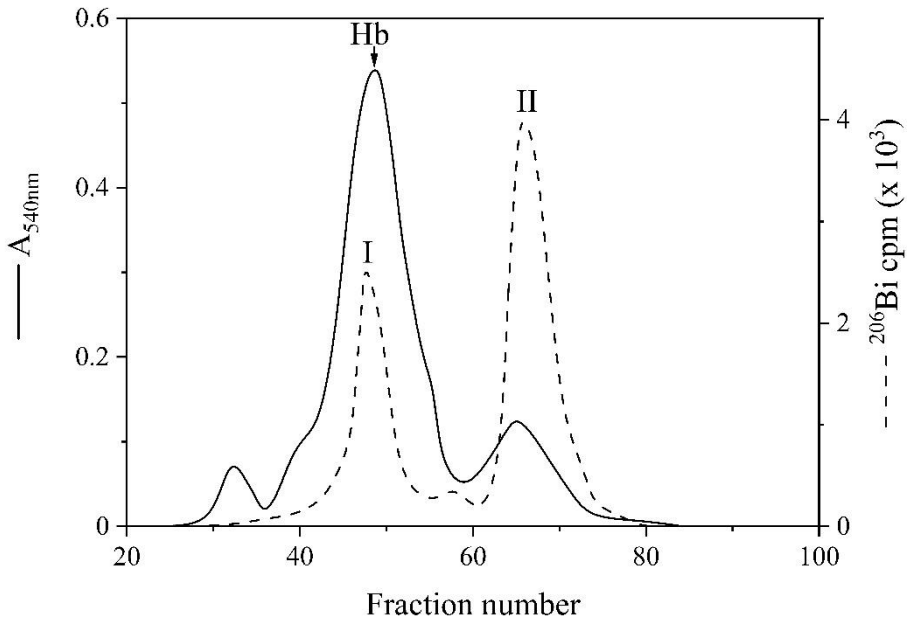

Fig.6 SEC of ^{206}Bi-containing RBC cytosol of rats 24 h after i.p. injection of 0.8 µg Bi kg^{-1} bw as $^{206}Bi(NO)_3$. Aliquots of the cytosol were fractionated on Sephadex G-150 column (2.5 cm x 100 cm) previously equilibrated with 5 mmol L^{-1} phosphate buffer, pH 8.0, using the same buffer as eluent. Recovery of applied ^{206}Bi: 87%. Hb: hemoglobin

Fractionation of the pooled and dialyzed ^{206}Bi-containing Hb fraction by acid acetone precipitation of globin followed by counting of ^{206}Bi in the precipitate (globin fraction) and supernatant (heme fraction) (Fig.1) showed that the radioactivity was almost entirely associated with the globin precipitate, with heme contributing for the 5% of the Bi of the total fraction (Table 2). This latter value was not large enough to suggest an incorporation of Bi into the heme moiety.

Subsequent resolution of globin fraction into α and ß polypeptide chains by chromatography on a CM-cellulose column (Fig.7) and counting of ^{206}Bi in the eluate showed one peak of ^{206}Bi associated with the UV absorbing ß chain identified as the molecular binding site for Bi in the globin (Table 2).

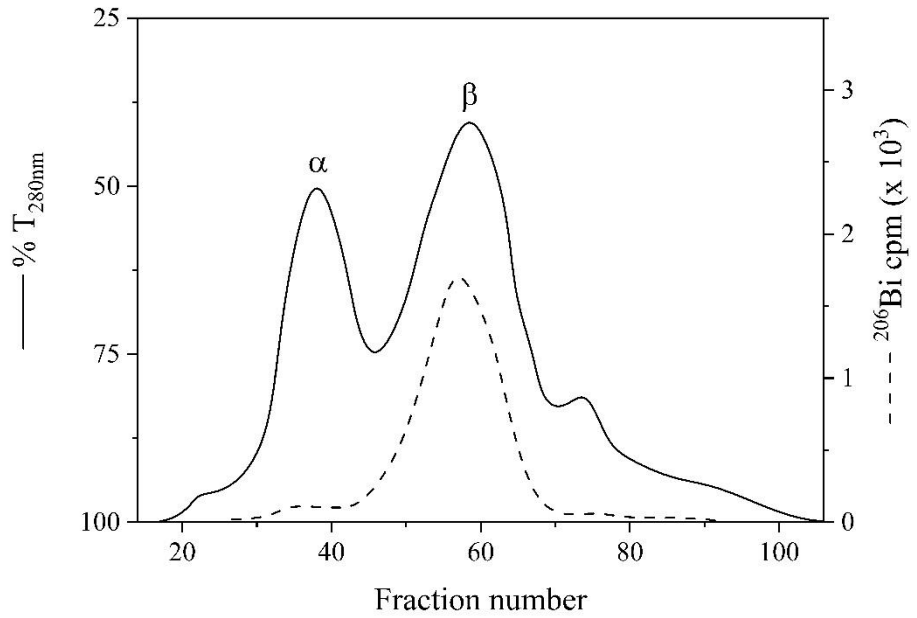

Fig.7 Separation of α and ß peptide chains of ^{206}Bi-containing globin. The protein was dissolved in a starting buffer (5 mmol L^{-1} Na_2HPO_4 and 50 mmol L^{-1} 2-mercaptoethanol in 8 mol L^{-1} urea solution, pH 6.8) and layered on a CM-cellulose column (2 cm x 20 cm) previously equilibrated with the same buffer. Elution of the chains was performed by a gradient of 0.005-0.05 mol L^{-1} Na_2HPO_4, pH 6.7 (see Section 2.7.5). Recovery of the applied radioactivity: 92%

3.4. Dialysis experiments

Less than 15% of Bi was removed from blood and various intracellular components by extensive dialysis against the buffers used in the fractionation processes (see Sections 2.6 and 2.7). The only exceptions concerned the whole RBC and RBC cytosol fractions, for which a statistically significant amounts ($p< 0.01$) of the initial ^{206}Bi in dialysis membrane were released by dialysis against the phosphate buffer used for RBC fractionation (Table 3). However, dialysis against acetate buffer at pH 5 or buffers used for plasma and RBC fractionation added with complexing agents (EDTA, citrate and particularly DMSA) efficiently removed the radioactivity from all biochemical samples dialyzed.

4. Discussion

In this paper we have investigated the metabolic fate of Bi in the blood of rats i.p. exposed to 0.8 µg Bi kg^{-1} bw. In order to place the present work in proper biochemical/toxicological context we believe crucial to comment the meaning of the adopted dose exposure. This was thousand times less than the high

(pharmacologically relevant) dose exposure which in literature characterize the bulk of the biochemical/toxicological information on Bi, given its main use in medicine for a very long time [5]. As the entity of the dose exposure to trace elements markedly affect their metabolism and biochemical effects [31] data on Bi metabolism at so high dose exposure are far from predicting its metabolic pathways at ultratrace levels of exposure. In addition, the few studies in which the metabolism of Bi was investigated by administering infinitesimal doses (NCA Bi-radiotracers, typically pg Bi kg^{-1} bw) are not entirely predictive. NCA radioisotopes can behave more like colloids than true solutes [49] leading to differences in their metabolic pathways compared to the same radioisotopes in carrier-added (CA) form [50]. For this, to give our study a real environmental toxicology connotation we selected the exposure at µg Bi kg^{-1} bw on the basis of criteria that define "dose exposure" of heavy metals which should be administered to laboratory animals as "environmental exposure levels" [31]. This premise is relevant because any comparison of our findings with the existing information of literature that follows must be interpreted with great caution, being mandatory in the comparison to specify doses and Bi species to which animals were exposed.

4.1. Distribution in the blood

In the present work, at 24 h post injection the blood-concentration of Bi was < 0.1% of the dose administered (Table 1). There are only two pioneering studies at infinitesimal dose exposure with which our result could be compared. Russ et al. [28] injected i.p 180 µCi of NCA ^{206}Bi- citrate into rats. 24 h later 0.07% of the injected radioactivity was found in the blood. Vienet et al. [30] recovered 0.006% of ^{206}Bi in the blood 24 h after i.v. injection of 10 µCi of NCA $^{206}Bi(NO)_3$ in the rat. However, both works were lacking information on the specific radioactivity of the injected ^{206}Bi radiotracer, making it impossible to establish the real concentration of the Bi mass to which animals were exposed.

In the blood, we found Bi distributed between RBC and plasma in a ratio of 2:1 (Table 2). Russ et al. [28] showed that after *in vitro* incubation of rat blood with ^{206}Bi-citrate 17% of the radioactivity was recovered

in the erythrocytes. However, another *in vitro* study indicated that in blood of the rat incubated with 25-5 000 ng Bi mL^{-1} as $Bi(NO)_3$ Bi was primarily present in RBC, with non-linear Bi RBC-to-plasma ratios ranging from 13 to 50.5 for the lower and upper doses incubated [51]. The non-linear nature of the binding of Bi to plasma proteins *in vitro* suggested that at low Bi plasma concentrations a smaller fraction of the element would be available for uptake by RBC than at higher concentrations [51]. In our work, the concentration of Bi in the blood (Table 1) was about 140 times lower than that (25 ng mL^{-1}) of Rao's work [51]. This may explain the divergent conclusion concerning the Bi repartition between RBC/plasma, indicating that great caution must be used in extrapolating *in vitro* data to an *in vivo* situation. Moreover, *in vivo* biokinetic factors would play a fundamental role in determining such repartition.

4.2. Distribution in the plasma

When ^{206}Bi-bearing plasma was subjected to SEC using Sephadex G-150 the elution pattern showed the association of Bi with four protein pools with different molecular sizes: (i) > 300 kDa; (ii) 160 kDa; 70 kDa and < 6.5 kDa (Fig.2). Bi was firmly protein-bound as suggested by: (i) the high recovery of ^{206}Bi (89% of total applied radioactivity) in the eluate from SEC (Fig.2), a separation process that can completely dissociate weak biocomplexes; (ii) extensive dialysis of the whole ^{206}Bi-plasma at physiological pH showing a modest release of ^{206}Bi (Table 3). As whole, the relative proportions of the eluted ^{206}Bi-complexed proteins and the minor percentage of Bi bound to LMWC (approx. 10% of the total Bi of the plasma, Table 2) indicated that Bi in the plasma was mainly bound to high molecular weight proteins, particularly to those of 160 kDa pool. No attempt has been done to identify Bi binding biomolecule(s) of protein pools with MW > 300 kDa (IgM, beta-lipoprotein, alpha 2-macroglobulin, haptoglobin fraction), 160 kDa (ceruloplasmin, IgE, IgG fraction) as well as < 6.5 kDa (LMWC, such as glutathione and single amino acids), this latter fraction representing the diffusible form of the plasma Bi at a rate of about 10% (Table 2). This is a noteworthy subject for future study. Instead, the 70 kDa pool of ^{206}Bi-containing proteins, principally transferrin/albumin, was subjected to a deepening to identify individual Bi- binding biomolecules. The

resolution was achieved by ion exchange chromatography on DEAE Sephadex A-50 that allowed the separation of the two proteins (Fig.3), and by an electrophoretic run, with the help of ^{59}Fe radiolabeling of iron proteins (Fig 4). As whole, for the first time we have demonstrated *in vivo* the binding of Bi with plasma transferrin. Until now, an "unexpected" binding of Bi to human serum/plasma transferrin and albumin was reported only by *in vitro* studies [52,53]. Our *in vivo* identification of transferrin as a carrier of Bi in blood plasma supports the thesis that the neurologic effects of Bi could be related to its passage of the blood-brain-barrier by the recognition of the transferrin receptor in the brain, in a similar manner to Al^{3+} [54]. Moreover, it has been suggested that transferrin would be the major target of Bi in human blood plasma, playing a role in the pharmacology of Bi [55]. Our findings are not in line with this suggestion. More than 60% of the Bi in the plasma was associated with HMWC other than transferrin (Table 2), this latter representing the 30% of the Bi bound to plasma proteins that may be responsible for the retention of Bi circulating in the blood.

4.3. Distribution in RBC

Examination of the intra-erythrocyte trafficking of Bi by separate analysis of the RBC after hemolysis and centrifugation showed that both the membrane (ghosts) and the cytosol were the erythrocyte-associated compartments for Bi binding, containing the second most relevant part of the RBC Bi (Table 2).

Fractionation of ^{206}Bi-ghosts-free cytosol by SEC on Sephadex G-150 (Fig.5) suggests that the binding of Bi would occur with more than one membrane protein pool. Such Bi-binding sites would be independent of lipids as suggested by dialysis of non-delipidated/delipidated membranes at physiological pH against the solubilizing buffer (Table 3). Moreover, extraction of lipids from the ^{206}Bi-ghosts showed that the amount of radioactivity extracted (Table 2) was not significant under our experimental conditions to suggest an association of Bi with membrane lipids.

Fractionation of ^{206}Bi-cytosol by SEC on Sephadex G-150 (separation of Hb and non-heme proteins, Fig.6) followed by acid acetone precipitation of globin as well as CM-cellulose chromatography (separation of α

and ß polypeptide globin chains, Fig.7) suggests that Bi which entered the RBC cytosol was distributed between non-hemoglobin LMWC and hemoglobin molecules in association with the ß chain of the globin. The identity of non-hemoglobin LMWC was not pursued and would be worthy of further research.

4.4. Dialysis experiments

Dialysis experiments were conducted to understand the strength (covalent or weaker binding) with which Bi was associated with blood components. At physiological pH an obvious amount of ^{206}Bi released was observed only for whole ^{206}Bi-RBC and its ghost free cytosol (Table 3). This can be explained by the presence of Bi-biocomplexes with molecular size < 6.5 kDa (approx. 64% of the total cytosolic ^{206}Bi, Table 2) in the cytosol. This size is lower than the size exclusion of the dialysis membrane (14 kDa) and therefore diffusible. Overall, the dialysis experiments suggest that Bi was strongly bound to biocomponents at physiological pH with a low degree of the breaking of Bi-complexes during the applications of the experimental protocols for their isolation. A confirmation comes from the high recoveries (80-90%) of the ^{206}Bi from SEC, ion exchange and CM-cellulose chromatography of the various ^{206}Bi-containing components. However, the Bi-biocomplexes were sensitive to acidic pH 5.0, and to the presence of complexing agents in the dialysis fluid at physiological pH, particularly of DMSA, for which Bi has an exceptionally high stability constant [56]. Our experiments did not exclude possible weaker associations of Bi with blood biocomponents in noncovalent form that could be dissociated during dialysis and chromatographic steps. Other specific methods such as equilibrium dialysis and Hummel and Dreyer [57] techniques would be used to detect them.

4.5. Distribution of Bi in the blood: comparative interpretation

As whole, the results obtained here allowed a punctual picture of the multi compartmental distribution of the ultratrace levels of Bi that circulated the blood 24 h after exposure leading to comparative

interpretations about the presence of the bismuth *de novo* incorporated into the different blood compartments and their subfractions (Fig.8).

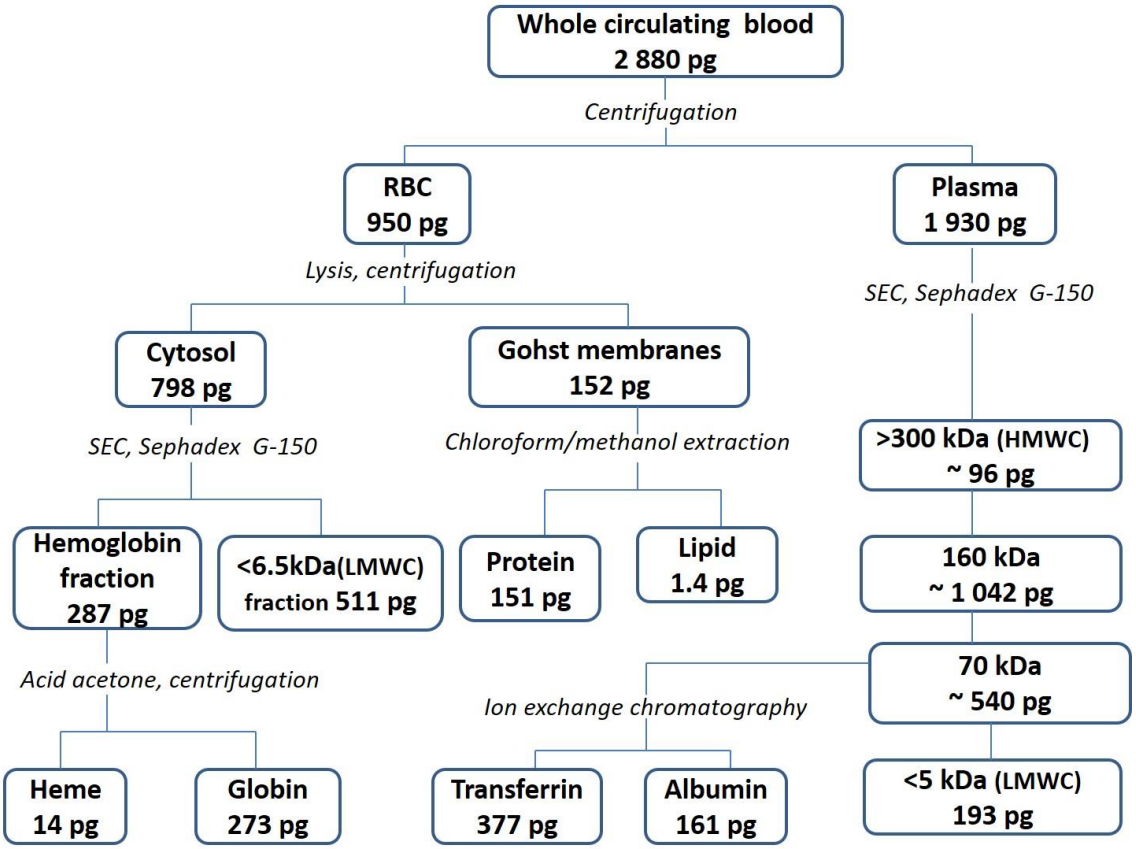

Fig.8 Estimation of the distribution of Bi among blood components of the rat 24 hours after the i.p. injection of 0.8 µg Bi kg^{-1} bw as $^{206}Bi(NO)_3$. Results are expressed in absolute total pg of Bi in each blood fraction considered. The calculations were based on the blood concentration of Bi determined experimentally (Table 1) in relation to the relative percentage of the repartition of Bi among blood components (Table 2), and assuming 16 mL per rat as average volume of circulating blood [58]. In italic: methods of fractionations

The bismuth in the blood was partitioned between plasma, the compartment with the major amount of the element, and RBC. In plasma, bismuth exhibited high affinity for proteins. Four pools of proteins with different molecular weight were identified as bismuth binders, representing the association with 160 000 kDa components the major Bi-binding pool followed by the 70 kDa transferrin-albumin pool. The high molecular weight of the most of protein-bound bismuth pools was an index of its non-diffusible form, representing the Bi-low molecular weight (LMWC) complexes (diffusible pool) a tenth of the plasma-bismuth.

The bismuth interacted with RBC, being mostly penetrating through the cell membranes, appearing to be (cytosolic) rather than bound to ghost membranes where was associated to proteins, not to lipids. Intracellularly, bismuth in RBC was recovered as two biochemical pools. The first predominating Bi-pool was represented by Bi-LMWC complexes. The second was identified as Bi-bound hemoglobin pool where the element was in combination with the polypeptidic ß chain of the globin, rather than with the heme group.

In summary the comparative analysis of the data concerning the multi compartmental distribution of bismuth in the blood (Fig.8) suggests that the element in blood plasma and blood RBC would exist not as a single entity but in form of different biochemical pools. This could be explained by the different affinity of bismuth for blood plasma and cell biomolecules, resulting in a complex process.

Although we are fully aware that the estimates have an indicative value, they still offer many insights for orienting future research in the area of study. The present study, however, presents some limitations, from which we can draw ideas for future research: (i) it is a snapshot at a single dose and exposure time. Biokinetic investigations at increasing dose exposure of bismuth are needed to identify the timed distribution among blood components, and to understand how the dose exposure affects its distribution; (ii) the radiochemical approach here developed based on the use of ^{206}Bi made it possible to establish the total concentrations of bismuth incorporated *de novo* in the various blood components. Speciation studies are necessary to establish if bismuth has undergone biotransformations, and to identify other specific Bi-binding components.

5. Conclusions

At the best of our knowledge the present work is the first *in vivo* study, on the basis of an environmental toxicology approach, aiming at describing the metabolic fate of Bi in the blood of rats at intracellular and molecular levels. As whole our study is of interest in improving understanding of the mechanism of

bismuth transport in the body and in providing a basis for the design of more effective Bi-based agents in health care.

The increasing industrial and medical applications of Bi and the advent of the “nano-era” with the great emerging potential applications of bismuth-based nanoparticles has given impetus for the present work. We hope it may serve as a stimulus in awakening attention to Bi in the area of the biochemistry and toxicology concerning long term-low dose exposure which are typical of environmental and occupational exposure in the present industrial society [32].

Contributorship

Sabbioni: Conceptualization, Writing - Original draft, Resources, Supervision, Investigation

Groppi: Investigation, Funding acquisition

Di Gioacchino: Writing - Review & Editing, Supervision

Petrarca: Writing Review & Editing, Visualization

Manenti: Investigation, Formal analysis, Visualization, Writing - Review & Editing

Declaration of Competing Interest

The authors declare that they have no conflicts of interest.

Acknowledgment

We are grateful to Mrs. J.Edel for the excellent technical assistance with the work of laboratory animals and gel filtration experiments. We also like to thank Messrs R.Pietra and G. Tettamanti (Ascom, Milan) for the assistance with the radioactive counting by γ-ray spectrometry.

Special thanks to Dott. Lorenzo Vilona for his contribution in reviewing the English language of the manuscript

References

1. Ying Zhou, Fan Dong, Shengming Jin (Eds.), Bismuth - Advanced Applications and Defects Characterization (Abs)June 2018 https:// doi: 10.5772/intechopen.71174

2. Filella, M. How reliable are environmental data on 'orphan' elements? The case of bismuth concentrations in surface waters. J. Environ. Monit., 2010, 12, 90-109

3. Phuoc Huu Le, Nguyen Trung Kien and Chien Nguyen Van (June 20th 2018). Recent Advances in BiVO4- and Bi2Te3-Based Materials for High Efficiency-Energy Applications, Bismuth - Advanced Applications and Defects Characterization, Zhou Y., Dong F., Jin S., IntechOpen, DOI: 10.5772/intechopen.75613. Available from: https://www.intechopen.com/books/bismuth-advanced-applications-and-defects-characterization/recent-advances-in-bivo4-and-bi2te3-based-materials-for-high-efficiency-energy-applications

4. Minh Thang Le (November 5th 2018). Bismuth Molybdate-Based Catalysts for Selective Oxidation of Hydrocarbons, Bismuth - Advanced Applications and Defects Characterization, Zhou Y., Dong F., Jin S., IntechOpen, DOI: 10.5772/intechopen.75105. Available from: https://www.intechopen.com/books/bismuth-advanced-applications-and-defects-characterization/bismuth-molybdate-based-catalysts-for-selective-oxidation-of-hydrocarbons

5. Wang R., Li H., Sun H. Bismuth: Environmental Pollution and Health Effects. Encyclopedia of Environmental Health. 2019;415-423. doi:10.1016/B978-0-12-409548-9.11870-6

6. Dolara P. Occurrence, exposure, effects, recommended intake and possible dietary use of selected trace compounds (aluminium, bismuth, cobalt, gold, lithium, nickel, silver). International Journal of Food Sciences and Nutrition, 2014; 65:8, 911-924, DOI: 10.3109/09637486.2014.937801

7. Borbinha, C., Serrazina, F., Salavisa, M. and Viana-Baptista M. Bismuth encephalopathy- a rare complication of long-standing use of bismuth subsalicylate. BMC Neurol 19, 212 (2019). https://doi.org/10.1186/s12883-019-1437-9

8. Thomas F., Bialek B., Hensel R. Medical Use of Bismuth: the Two Sides of the Coin. J Clinic Toxicol 2012; S3:004. doi:10.4172/2161-0495.S3-004

9. Keogan D.M., Griffith D.M. Current and potential applications of bismuth-based drugs. Molecules. 2014 Sep 23;19(9):15258-97. doi: 10.3390/molecules190915258

10. Yang N., Tanner J., Zheng B.-J., Watt R., He M.-L., Lu L.-Y., Jiang J.-Q., Shum K.-T., Lin Y.-P., Wong K.-L., Lin M., Kung H.-F., Sun H., Huang J.-D. Bismuth Complexes Inhibit the SARS Coronavirus. Angewandte Chemie International Edition, 2007; 46: 6464-6468. doi:10.1002/anie.200701021

11. Tafreshi N.K., Doligalski M.L., Tichacek C.J., Pandya D.N., Budzevich M.M., El-Haddad G., Khushalani N.I., Moros E.G., McLaughlin M.L., Wadas T.J., Morse D.L. Development of Targeted Alpha Particle Therapy for Solid Tumors. Molecules 2019, 24, 4314.

12. Reverberi A.P., Vocciante M., Salerno M., Caratto V., Fabiano, B. Bi Nanoparticles Synthesis by a Bottom-up Wet Chemical Process. Chemical Engineering Transactions. 2019; 73:283-288. DOI: 10.3303/CET1973048

13. Shahbazi M., Faghfouri L., Ferreira M.P.A., Figueiredo P., Maleki H., Sefat F., Hirvonen J., Santos H.A. The versatile biomedical applications of bismuth-based nanoparticles and composites: therapeutic, diagnostic, biosensing, and regenerative properties. Chem. Soc. Rev., 2020, 49, 1253-1321 DOI: 10.1039/C9CS00283A

14. Anku W.W., Oppong S.O.B, Govender P.P. (2018). Bismuth-Based Nanoparticles as Photocatalytic Materials, In: Bismuth - Advanced Applications and Defects Characterization, Zhou Y., Dong F., Jin S., IntechOpen, DOI: 10.5772/intechopen.75104

15. Naasz S., Weigel S., Borovinskaya O., Serva A., Cascio C., Undas A.K., Simeone F.C., Marvin H.J.P., Peters R.J.B. Multi-element analysis of single nanoparticles by ICP-MS using quadrupole and time-of-flight technologies J. Anal. At. Spectrom., 2018,33, 835-845 https://doi.org/10.1039/C7JA00399D

16. Esquivel-Gaon M., Anguissola S., Garry D., Gallegos-Melgar A.D.C., Saldaña J.M., Dawson K.A., De Vizcaya-Ruiz A., Del Razo L.M., Bismuth-based nanoparticles as the environmentally friendly replacement for lead-based piezoelectrics RSC Adv., 2015, 5, 27295-27304 DOI: 10.1039/C5RA02151K

17. Zaccariello G., Back M., Zanello M., Canton P., Cattaruzza E., Riello P., Alimonti A., Benedetti A. Formation and Controlled Growth of Bismuth Titanate Phases into Mesoporous Silica Nanoparticles: An Efficient Self-Sealing Nanosystem for UV Filtering in Cosmetic Formulation ACS Appl. Mater. Interfaces 2017, 9, 2, 1913–1921 https://doi.org/10.1021/acsami.6b13252

18. Li Z., Hu Y., Miao Z., Xu H., Li C., Zhao Y., Li Z., Chang M., Ma Z., Sun Y., Besenbacher F., Huang P., Yu, M. Dual-Stimuli Responsive Bismuth Nanoraspberries for Multimodal Imaging and Combined Cancer Therapy. Nano Lett., 2018, 18, 6778–6788 https://doi.org/10.1021/acs.nanolett.8b02639

19. Cheng X., Yong Y., Dai Y., Song X., Yang G., Pan Y., Ge C. Enhanced Radiotherapy using Bismuth Sulfide Nanoagents Combined with Photo-thermal Treatment. Theranostics 2017; 7(17):4087-4098. doi:10.7150/thno.20548. Available from http://www.thno.org/v07p4087.htm

20. Torrisi L., Restuccia N., Silipigni L., Cuzzocrea S., Cordaro M. Synthesis of bismuth nanoparticles for biomedical applications In: Proceedings of the international workshop on NEW APPROACHES TO STUDY COMPLEX SYSTEMS (Messina, Italy; 27-28 November 2017), Caccamo M.T., Magazù S., Pasqua L. and Restuccia L. eds, Vol 97, N_O S2, A12 (2019) https://doi.org/10.1478/AAPP.97S2A12

21. Mishra V., Baranwal V., Mishra R.K., Sharma S., Paul B., Pandey A.C. Immunotoxicological impact and biodistribution assessment of bismuth selenide (Bi_2Se_3) nanoparticles following intratracheal instillation in mice. Sci Rep. 2017; (1):18032 doi:10.1038/s41598-017-18126-y

22. Jassim A.M.N., Ahmed F., Jehan A., Khawla K., Al Marjani M.F., Mohammed M. Study the Antibacterial Effect of Bismuth Oxide and Tellurium Nanoparticles. International journal of chemical and biomolecular science, 2015; 1:81-84.

23. C. Khatua, S. Bodhak, B. Kundu and V. K. Balla, In vitro bioactivity and bone mineralization of bismuth ferrite reinforced bioactive glass composites. Materialia, 2018; 4:361–366

24. Bi, H.; He, F.; Dong, Y.; Yang, D.; Dai, Y.; Xu, L.; Lv, R.; Gai, S.; Yang, P. & Lin, J. Bismuth Nanoparticles with "Light" Property Served as a Multifunctional Probe for X-ray Computed Tomography and Fluorescence Imaging Chemistry of Materials, 2018, 30, 3301-3307 https://doi.org/10.1021/acs.chemmater.8b00565

25. Winter H., Brown A.L., Goforth A.M. (June 20th 2018) Bismuth-Based Nano- and Microparticles in X-Ray Contrast, Radiation Therapy, and Radiation Shielding Applications, Bismuth - Advanced Applications and Defects Characterization, Zhou Y., Dong F., Jin S., IntechOpen, DOI: 10.5772/intechopen.76413. Available from: https://www.intechopen.com/books/bismuth-advanced-applications-and-defects-characterization/bismuth-based-nano-and-microparticles-in-x-ray-contrast-radiation-therapy-and-radiation-shielding-ap

26. Slikkerveer A., de Wolff F.A., Pharmacokinetics and Toxicity of Bismuth Compounds. Med Toxicol Adverse Drug Exp 1989; 4:303–323. https://doi.org/10.1007/BF03259915

27. Durbin P.W. Metabolic characteristics within a chemical family. Health Phys. 1960; 2:225-238. doi:10.1097/00004032-195907000-00001

28. Russ G.A., Bigler R.E., Tilbury R.S., Woodard H.Q., Laughlin J.S. Metabolic studies with radiobismuth. I. Retention and distribution of ^{206}Bi in the normal rat. Radiat Res. 1975; 63(3): 443-454.

29. Zidenberg-Cherr S., Parks N.J., Keen C.L. Tissue and subcellular distribution of bismuth radiotracer in the rat: considerations of cytotoxicity and microdosimetry for bismuth radiopharmaceuticals. Radiat Res. 1987; 111(1):119-129.

30. Vienet R., Bouvet P., Istin M. Cinétique et distribution du ^{206}Bi chez le rat et le lapin: un modèle. Int J Appl Radiat Isot. 1983; 34(4):747-753. doi:10.1016/0020-708x(83)90255-7

31. Sabbioni E., Goetz L., Birattari C., Bonardi M. Environmental biochemistry of current environmental levels of heavy metals: preparation of radiotracers with very high specific radioactivity for metallobiochemical experiments on laboratory animals. Sci Total Environ. 1981; 17(3):257-276.

32. Sabbioni E., Di Gioacchino M., Farina M., Groppi F., Manenti S. Radioanalytical and nuclear techniques in trace metal toxicology research. J Radioanal Nucl Chem 2018; 318:1749–1763. https://doi.org/10.1007/s10967-018-6321-3

33. Casteleyn K., Castiglioni M., Manes L., Weckermann B. Production of radionuclides at the JRC-Ispra cyclotron. J. Trace Microprobe Tech., 1993; 11:13-27

34. Acerbi E., Birattari C., Castiglioni M., Resmini F., Nuclear applied physics at the Milan Cyclotron. J. Radioanal. Chem. 1976; 34: 191–217 https://doi.org/10.1007/BF02521521

35. Birattari C., Bonardi M., Gilardi M.C., Production of bismuth radiotracers in the Milan AVF cyclotron for environmental toxicology and proton activation analysis. Radiochem. Radioanal. Lett. 1981; 49:25-36

36. Adsul J.S., Dias C.C., Iyer S.G., Venkateswarlu C., Use of Chelex 100 in determination of bismuth in sulphide ores, concentrates, metals and alloys. Talanta. 1987; 34(5):503-504. doi:10.1016/0039-9140(87)80169-8

37. Schramel P., Wendler I., Angerer J. The determination of metals (antimony, bismuth, lead, cadmium, mercury, palladium, platinum, tellurium, thallium, tin and tungsten) in urine samples by inductively coupled plasma-mass spectrometry. Int Arch Occup Environ Health 1997; 69:219–223 https://doi.org/10.1007/s004200050140

38. Sabbioni E., Fortaner S., Manenti S., Groppi F., Bonardi M., Bosisio S., Di Gioacchino M. The metallobiochemistry of ultratrace levels of platinum group elements in the rat. Metallomics, 2015,7, 267-276

39. Bosisio S., Fortaner S., Rizzio E., Groppi F., Salvini A., Bode P., Wolterbeek B., Di Gioacchino M., Sabbioni E. Nuclear and spectrochemical techniques in developmental metaltoxicology research. Whole-body elemental composition of Xenopus laevis larvae. J.Radioanal Nucl Chem 2015; 303:2127-2134 DOI: 10.1007/s10967-014-3792-8

40. EU, Directive 86/609/EEC of 24 November 1986 on the approximation of laws, regulations and administrative provisions of the Member States regarding the protection of animals used for experimental and other scientific purposes. Official Journal of the European Community L358 (1986) 1-29.

41. Sabbioni E., Fortaner S., Bosisio S., Farina M., Del Torchio R., Edel J., Fischbach M. Metabolic fate of ultratrace levels of $GeCl_4$ in the rat and in vitro studies on its basal cytotoxicity and carcinogenic potential in Balb/3T3 and HaCaT cell lines. J. Appl. Toxicol., 2010; 30: 34-41. doi:10.1002/jat.1469

42. Dodge J.T., Mitchell C., Hanahan D.J. The preparation and chemical characteristics of hemoglobin-free ghosts of human erythrocytes. Arch Biochem Biophys. 1963; 100:119-130. doi:10.1016/0003-9861(63)90042-0

43. Grimsley, G. R., & Pace, C. N. Spectrophotometric Determination of Protein Concentration. Current Protocols in Protein Science, 2003 3.1.1–3.1.9. doi:10.1002/0471140864.ps0301s33

44. Folch J., Lees M., Stanley G.H.S. A simple method for the isolation and purification of total lipides from animal tissues. J Biol Chem. 1957; 226(1):497–50 https://doi.org/10.1007/978-94-007-7864-1_89-1

45. Bornens M., Kasper C.B. Fractionation and partial characterization of proteins of the bileaflet nuclear membrane from rat liver. J Biol Chem. 1973; 248(2):571-579.

46. Eilers, R.J. Notification of final adoption of an international method and standard solution for hemoglobinornetry specifications for preparation of standard solution. Am. J. Clin. Pathol. 1967; 47: 212-214.

47. Winterhalter K.H., Huenhs E.R. Preparations, properties, and specific recombination of alpha-beta-globin subunits. The Journal of Biological Chemistry, 1964; 239:3699– 3705.

48. Crkvenjakov R., Cusić S., Ivanović, I., Glisin, V. Rat b/b Anemia: Translation of Normal and Anemic Globin mRNA in Wheat-Germ Cell-Free System. European journal of biochemistry, 1977; 71: 85-91. 10.1111/j.1432-1033.1976.tb11092.x.

49. Luckey T.D., Venugopal B. Metal toxicity in mammals.Physiologic and Chemical Basis for Metal Toxicity vol1 chapter 4,p.110, Plenum Press, 1977

50. Coenegracht J.M., Dorleyn M. The distribution of intravenously administered tracer doses of Bi-206 compounds in the human body. Journal Beige de Radiologie, 44: 485-504, 1961

51. Rao N., Feldman S. Disposition of bismuth in the rat. I. Red blood cell and plasma protein binding. Pharm Res. 1990;7(2):188-191. doi:10.1023/a:1015841105215

52. Li H., Sadler P. J., Sun H. Unexpectedly strong binding of a large metal ion Bi^{3+} to human serum transferrin. J. Biol. Chem. 1996; 271: 9483–9489.

53. Sun H., Li H., Mason A.B., Woodworth R.C., Sadler P.J. Competitive binding of bismuth to transferrin and albumin in aqueous solution and in blood plasma. J Biol Chem. 2001;276(12):8829-8835. doi:10.1074/jbc.M004779200

54. Roskams A.J., Connor J.R. Aluminum access to the brain: a role for transferrin and its receptor. Proceedings of the National Academy of Sciences Nov 1990, 87 (22) 9024-9027. doi:10.1073/pnas.87.22.9024

55. Sun H., Szeto K.Y. Binding of bismuth to serum proteins: implication for targets of Bi(III) in blood plasma. J Inorg Biochem. 2003; 94(1-2):114-120. doi:10.1016/s0162-0134(02)00649-9

56. Wesley R.H., Yong C., Jana S., Bharat S. Stability Constants for Dimercaptosuccinic Acid with Bismuth(III), Zinc(II), and Lead(II), Journal of Coordination Chemistry, 1991; 23:1-4, 173-186, DOI: 10.1080/00958979109408249

57. Berger G., Girault G. Macromolecule-ligand binding studied by the Hummel and Dreyer method: current state of the methodology. J Chromatogr B Analyt Technol Biomed Life Sci. 2003; 797(1-2):51-61. doi:10.1016/s1570-0232(03)00482-3

58. Lee H.B., Blaufox M.D. Blood volume in the rat. J Nucl Med. 1985 26:72-6. PMID: 3965655.